

Solving the relativistic hydrodynamic equation in presence of magnetic field for phase transition in a neutron star

Ritam Mallick

Department of Physics, Indian Institute of Science, Bangalore 560012, INDIA

Rajesh Gopal, Sanjay k Ghosh, Sibaji Raha

Centre for Astroparticle Physics and Space Science; Bose Institute; Block - EN, Sector V; Salt Lake; Kolkata - 700091; INDIA

Suparna Roychowdhury

Department of Physics; St. Xaviers College; Kolkata - 700016; INDIA

Abstract

Phase transition, from normal nuclear matter to quark matter, can take place inside a neutron star (NS) whose central density is of the order of 5-10 times normal nuclear matter saturation density (n_0). The transition is conjectured to occur via a conversion front, converting the neutron star to strange star. In this paper, we solve the relativistic hydrodynamic equations in presence of high magnetic field, usually present in NSs, for the conversion front. We have included the lorentz force due to magnetic field in the energy momentum tensor by averaging over the polar angles. We find that for a initial dipolar field configuration of the magnetic field with a sufficiently high value at the surface, increases the velocity of the front considerably.

Keywords: stars: neutron, stars: magnetic fields, equation of state, special relativity

Email addresses: ritam@physics.iisc.ernet.in (Ritam Mallick),
rajesh@bosemain.boseinst.ac.in (Rajesh Gopal)

1. Introduction

Normal nuclear matter and its interaction at high density and/or temperature is a area of current interest. As proposed by [1, 2] a form of matter consisting of almost equal numbers of up (u), down (d) and strange (s) quarks, may be the true ground state of strongly interacting matter. This conjecture is supported by Bag model calculations [3] for certain range of values for the strange quark mass and the strong coupling constant. Such bulk matter consisting of quarks was referred as "strange quark matter (SQM)". If the hypothesis is true then normal nuclear matter at high enough density and/or temperature, would be unstable.

Such extreme condition is beleived to occur in at least two scenarios; one being the production of the required extreme condition in the laboratory and analyzing them and the other being the indirect astrophysical tests, signals coming from dense compact stars. Some advancement has already been made to recreate the deconfinement transition in the collision of heavy nuclei in high energy accelerators *e.g.* at CERN-SPS in Geneva and RHIC in Brookhaven national laboratory (BNL). Along with the above man made laboratories, the compact stars having central density as high as 3-10 times nuclear matter saturation density, can be used to test nature of strongly interacting matter.

High density in NSs may induce a transition to quark matter, as SQM may be the true ground state of strongly interacting matter, as conjectured by Witten [1]. If this is true then there is a possibility that some NSs getting converted to quark star (QS), also sometimes referred as strange stars (SS), or at least hybrid star (HS). HSs are stars which are assumed to have a quark core surrounded by normal nuclear matter. Some tentative SS candidates are the compact objects associated with X-ray bursters GRO *J*1744–28 [4], SAX *J*1808.4 – 3658 [5] and X-ray pulsars Her *X* – 1 [6].

A few possible mechanisms for the production of SQM in a neutron star have been discussed by Alcock et al [7]. The conversion from hadron matter to quark matter is expected to start as the star comes in contact with a seed of external strange quark nugget. Another mechanism for the initiation of the conversion process was given by Glendenning ([8]). It was suggested that a sudden spin down of the star may increase the density at its core thereby triggering the conversion process spontaneously.

Conversion of neutron matter to strange matter has been studied by several authors. Olinto [9] viewed the conversion process to proceed via weak

interactions as a propagating slow-combustion (i.e. a deflagration) front and derived the velocity of such a front. Olesen and Madsen [10] and Heiselberg et al. [11] estimated the speed of such conversion front to range between 10 m/s to 100 km/s. Collins and Perry [12], on the other hand, assumed that the hadronic matter gets converted first to a two-flavour quark matter that eventually decays to a three-flavour strange matter through weak interactions. Horvath and Benvenuto [13] examined the hydrodynamic stability of the combustive conversion in a non-relativistic framework. In a relativistic framework, Cho et al [14] examined the conservation of the energy-momentum and the baryonic density flux across the conversion front. Recently, Tokareva et al [15] modeled the hadron to SQM conversion process as a single step process. Berezhiani et al. [16], Bombaci et al. [17] and Drago et al. [18], on the other hand, suggest that the formation of SQM may be delayed if the deconfinement process takes place through a first order transition [19] so that the purely hadronic star can spend some time as a metastable object.

Most of the papers have ignored some essential features of NS, namely the rotational effect, the general relativistic (GR) effect. We have systematically tried to incorporate these effects in a series of works. In Ref. [20], we have shown that the conversion process is most likely a two-step process. Following Glendenning we heuristically assumed the existence of conversion front originated at the centre and propagating outward through the star. The first step involves the conversion of NS to a two-flavour QS. We assumed that the central density to be high (3 – 10) times normal matter density, and the transition front proceeds as a detonation. Within a few millisecond the NS gets converted to a metastable 2-flavour QS. The second step comprises the conversion from two-flavour quark matter to the stable three-flavour SQM, through weak interaction. In our more recent work [21], we have exhibited the major role played by the GR effects in the rotating stars; the conversion fronts propagate with different velocities along different radial directions.

One of the most important characteristic of NS which we have still not incorporated is the magnetic fields. NS are also characterized by very high magnetic fields ($10^{10} - 10^{12}$ G) at the surface. While the origin of such magnetic fields in NS remains unclear (trapping of all magnetic lines of force during the collapse [22] can barely yield $10^8 - 10^9$ G), the observed slow-down rate of pulsars, which are rotating NS, do require such magnetic fields. Thus, the canonical picture of the classical pulsar mechanism involves [22] a magnetic dipole at the center of a rotating NS. In the present work, we report the findings after the incorporation of the magnetic field in the rel-

ativistic hydrodynamic equations. We actually solve the special relativistic hydrodynamic equations with the consideration that viscosity and resistivity are zero, that is an ideal hydrodynamic approximation.

To study the conversion process, we here consider relativistic EOSs describing the forms of the matter in respective phases. Due to the propagation of the shock wave, the properties of the medium on either side of the shock exhibit a discontinuity. Along with such EOS, we would also consider equations depicting various conservation conditions on either side of the front. Development of the conversion front, as it propagates radially through the model star in the presence of magnetic field, would be examined. In section II, we discuss the EOSs and the initial jump conditions. In section III, we present the governing equations for the combustion front propagation by incorporating the effect of the Lorentz force due to the magnetic field. In section IV, we present the results obtained by solving the relativistic MHD equations. Conclusions that may be drawn from these results are presented in the final section.

2. Initial jump condition

The nuclear matter phase is described by the non-linear Walecka model [23] and the quark phase by the MIT Bag model [24]. We treat both the nuclear and quark phases as ideal fluids. We take the picture of Glendenning [8] and assume that the phase transition was initiated by a sudden spin down of the star. So consider the physical situation where a combustion front has been generated in the core of the Neutron star. This front propagates outwards through the neutron star with a certain hydrodynamic velocity, leaving behind a u-d-e matter. We denote all the physical quantities in the hadronic sector by subscript 1 and those in the quark sector by subscript 2.

Quantities on opposite sides of the front are related through the energy density, the momentum density and the baryon number density flux conservation [15, 25, 26]. In the rest frame of the combustion front, the velocities of the matter in the two phases, are written as [25]:

$$v_1^2 = \frac{(p_2 - p_1)(\epsilon_2 + p_1)}{(\epsilon_2 - \epsilon_1)(\epsilon_1 + p_2)}, \quad (1)$$

and

$$v_2^2 = \frac{(p_2 - p_1)(\epsilon_1 + p_2)}{(\epsilon_2 - \epsilon_1)(\epsilon_2 + p_1)}. \quad (2)$$

3. Propagation of combustion front in the presence of Magnetic field

The preceding discussion is mainly a feasibility study for the possible generation of the combustive phase transition front. Using it to be the initial condition, we now study the evolution of the hydrodynamical combustion front with position in the presence of magnetic field. Following our recent work [20], we choose a regime where the propagation front moves as a detonation front. To examine such an evolution, we move to a reference frame in which the nuclear matter is at rest. The speed of the combustion front in such a frame is given by $v_f = -v_1$ with v_1 being the velocity of the nuclear matter in the rest frame of the front.

In this section we study the time evolution of the shock front within the special relativistic formalism in the presence of the static background magnetic field in the neutron star. The energy momentum tensor of an ideal fluid in the presence of a magnetic field can be written as the sum of the matter energy momentum tensor $T_{\mu\nu}^M$ and the magnetic energy momentum tensor $T_{\mu\nu}^B$. The matter energy momentum tensor can be written as:

$$T_{\mu\nu}^M = (p + \epsilon) u_\mu u_\nu + p \eta_{\mu\nu}$$

where, the fluid four velocity is $u_\mu = \Gamma(1, \vec{v})$, Γ is the Lorentz factor and \vec{v} is the fluid three velocity. The pressure and energy density p and ϵ are evaluated in the rest frame of the fluid.

The magnetic energy momentum tensor can be written in terms of its components as:

$$\begin{aligned} T_{00} &= \frac{B^2}{8\pi} \\ T_{0i} &= 0 \\ T_{ij} &= \frac{B^2}{8\pi} \delta_{ij} - \frac{B_i B_j}{4\pi} \end{aligned}$$

In writing down the components of the magnetic tensor, we have assumed that the electric field is zero in the nuclear matter rest frame. Hence T_{0i} which is simply the Poynting flux vector is zero. The equations of motion follow from the covariant conservation of the total energy momentum tensor $\partial_\nu T_T^{\mu\nu} = 0$. Thus we can write, $\partial_\nu T_{\mu\nu}^M = -\partial_\nu T_{\mu\nu}^B$. The expression on the right hand side in the above expression is simply the Lorentz four force f^μ . The zeroth component of the four force f^0 is zero since there is no

electric fields whereas the three-force is the Lorentz force due to magnetic field $\vec{F} = (\nabla \times \vec{B}) \times \vec{B}$.

Using the above arguments we can write down the hydrodynamic equation for the propagation of the transition front [20] in the presence of the magnetic field:

$$\frac{1}{\omega} \left(\frac{\partial \epsilon}{\partial \tau} + v \frac{\partial \epsilon}{\partial r} \right) + \frac{1}{W^2} \left(\frac{\partial v}{\partial \tau} + v \frac{\partial v}{\partial r} \right) + 2 \frac{v}{r} = 0 \quad (3)$$

and

$$\frac{1}{\omega} \left(\frac{\partial p}{\partial r} + v \frac{\partial p}{\partial \tau} \right) + \frac{1}{W^2} \left(\frac{\partial v}{\partial \tau} + v \frac{\partial v}{\partial r} \right) = \frac{\langle F_r \rangle}{4\pi\omega}, \quad (4)$$

where, $v = \frac{\partial r}{\partial \tau}$ is the front velocity in the nuclear matter rest frame and $k = \frac{\partial p}{\partial \epsilon}$ is taken as the square of the effective sound speed in the medium. p , ϵ , ω and W are the pressure, energy density, enthalpy and lorentz factor respectively.

We see that the effect of magnetic fields is included through the Lorentz force in eqn. 2. The energy equation is unaffected since we assume that the conductivity is formally infinite so that there are no energy dissipative effects. It is also to be noted that we have included the Lorentz force by considering its average over the polar angles. The Lorentz force term is not spherically symmetric. As a result, the shock speed would also vary with direction. As we are concerned only with the radial propagation (spherically symmetric star), and to keep some information of the assymetry part we have considered approximate angle averages. The details of the different configurations and the corresponding forms for the Lorentz force are detailed in the Appendix.

Equations (3) and (4) can be rewritten as:

$$\frac{2v}{\omega} \frac{\partial \epsilon}{\partial r} + \frac{1}{W^2} \frac{\partial v}{\partial r} (1 + v^2) + \frac{2v}{r} = 0 \quad (5)$$

and

$$\frac{n}{\omega} \frac{\partial \epsilon}{\partial r} (1 + v^2) + \frac{2v}{W^2} \frac{\partial v}{\partial r} = \frac{\langle F_r \rangle}{4\pi\omega} \quad (6)$$

We finally get a single differential equation for the front velocity:

$$\frac{dv}{dr} = \frac{1}{W^2 [4v^2 - k(1 + v^2)^2]} \left[\frac{\langle F_r \rangle}{4\pi\omega} + \frac{k(1 + v^2)}{r} \right] \quad (7)$$

The above equation is integrated with respect to r from the center to the surface. The initial velocity is fixed through the jump conditions for

different values of the central densities. The magnetic field is incorporated by specifying different configurations.

4. Results and Discussion

Equations (1) and (2) specify the respective flow velocities v_1 and v_2 of the nuclear and quark matter in the rest frame of the front. This would give us the initial velocity of the front ($-v_1$), at a radius infinitesimally close to the center of the star, in the nuclear matter rest frame. The nuclear matter EOS (walecka model) have been used to construct the static configuration of compact star, for different central densities, by using the standard Tolman-Oppenheimer-Volkoff (TOV) equations [27, 28]. The velocity at the center of the star should be zero from symmetry considerations. On the other hand, the $1/r$ dependence of the $\frac{dv}{dr}$, in eq. (7) suggests a steep rise in velocity near the center of the star. Equation (7) is then integrated, with respect to r , starting from the center towards the surface of the star. The solution gives us the variation of the velocity with the position as a function of time of arrival of the front, along the radius of the star.

In this section, we present the results of the velocity profiles for different magnetic field strength for dipole configurations. We first consider a poloidal magnetic field which can be specified in terms of the field components as:

$$B_r = \frac{B_0 \sin \theta}{r^3}$$

$$B_\theta = \frac{2B_0 \cos \theta}{r^3}$$

In the magnetic field profile, r is the distance from the center while B_0 is related to the surface magnetic field B_S through $B_0 = B_S R^3$. The angle averaged Lorentz force $\langle F_r \rangle$ for this configuration is $\langle F_r \rangle = \frac{B_0^2}{12\pi r^7}$ as evaluated in the appendix.

In fig. 1, we show the propagation velocity of the conversion front along the radius of the star with a central density of 4 times nuclear matter saturation density. The solid curve denotes the SR calculation without the consideration of the magnetic field. The dotted curve is for SR calculation with a surface magnetic field of dipolar nature of strength 10^{10} Gauss. Below this field the effect of magnetic field on the conversion front is very negligible. The curve shows that the magnetic field enhances the velocity of the front which is also clear from equation (7). Next we increase the magnetic field

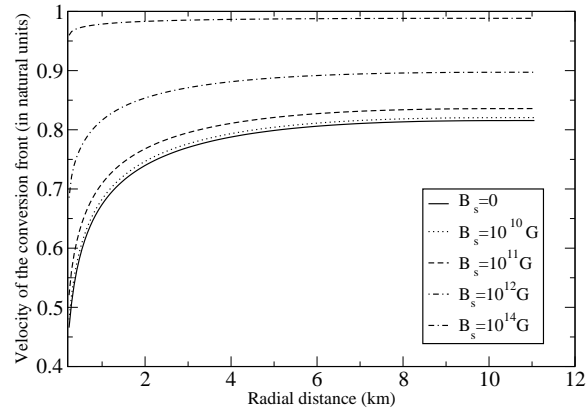


Figure 1: Variation of velocity of the conversion front along the radial distance of the star for various values of the surface magnetic field.

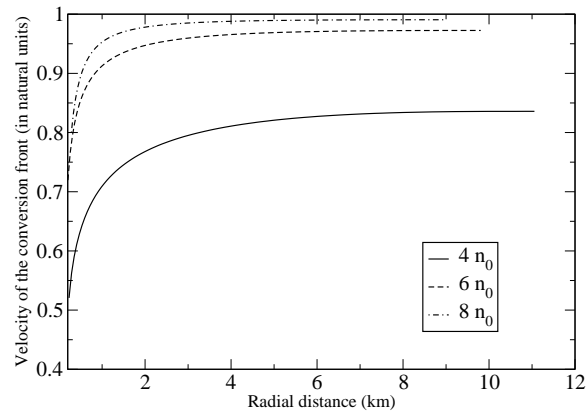


Figure 2: Variation of velocity of the conversion front along the radial direction with a surface magnetic field of strength of 10^{11} gauss for different values of the central density.

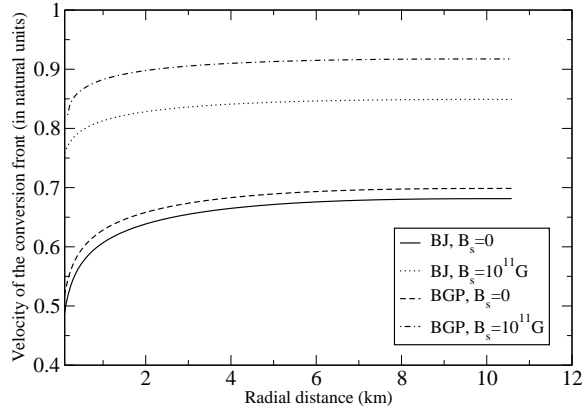


Figure 3: Variation of velocity of the conversion front along the radial direction with a surface magnetic field of strength 10^{11} gauss for two different EOS namely BGP and BJ.

strength and the subsequent curves on the figure shows that the velocity of the conversion front increases with the increase of field strength. For a field strength of 10^{14} gauss the velocity of the front goes very near the speed of light, but such high magnetic field strength is found only in the magnetars.

Fig. 2 shows the velocity of the conversion front along the radial direction of the star for different central densities of the star. The solid curve is for the central density of 4 times that of nuclear matter saturation density (n_0) with a surface magnetic field of 10^{11} gauss. Next we increase the central density, and the two other curve is for the central density of 6 times (broken curve) and 8 times (broken-dot curve) that of nuclear saturation density respectively. The curves are plotted for the same value of the surface magnetic field (10^{11} gauss). We find that as the central density increases the velocity of the propagating front also increases. This is due to the fact that the velocity of the front depends on the value of k (equation (7)). For a high central density the star is more compact and therefore k is much larger making the velocity to increase further.

Similar calculation with central density 4 times that of nuclear saturation density is done for two other different EOS, Bowers, Gleeson and Pedigo (BGP) model [29] and Bethe and Jhonson (BJ) model [30]. Fig. 3 shows the velocity of the front for these two models with and without the effect of magnetic field. The surface magnetic field applied for the two cases is same (10^{11} gauss). This is to compare the effect of magnetic field as well as

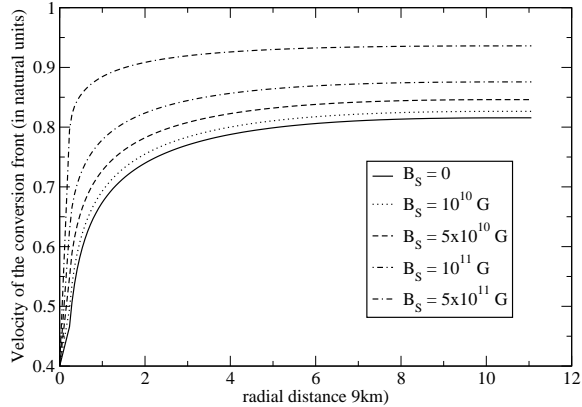


Figure 4: Variation of velocity of the conversion front along the radial direction for different magnetic field strength for toroidal field.

the effect of EOS on the velocity of the front. The magnetic field increases the velocity of the front similar to the previous curves. The BGP model is much steeper than the BJ model EOS, and by the reason given in the above paragraph the velocity of the front is larger for the BGP model than the BJ model. Therefore we find that the velocity of the front depends on the central density as well as the EOS we choose. The velocity increases with the increase in magnetic field. Below a certain value of the field the effect on the conversion front is not at all relevant and for a very high value of magnetic field (which may be found in magnetars) the velocity of the front attains a velocity close to that of the speed of light.

Little is known about the magnetic field structure in neutron star, and therefore it is not good enough to assume only poloidal field would be present there. A proto-neutron star dynamo [31] is unlikely to generate purely poloidal field and differential rotation will easily wrap any poloidal field and generate strong toroidal field [32]. Therefore it seems realistic to consider effect magnetic field configuration which consists of poloidal and toroidal components. The toroidal magnetic field grows from the poloidal dipole field. This can be possible if there is differential rotation in the star, which is usually present in a neutron star [33, 34]. The differential rotation of the star can be written as

$$V_d = r\hat{\phi}. \quad (8)$$

The toroidal field B_T due to this differential rotation and the dipole field is

given by

$$B_T = \nabla \times (V_d \times B) \quad (9)$$

where B is the dipole field. The toroidal field comes out to be

$$B_T = -\frac{B_0 \sin\theta}{r^3} \hat{\phi} \quad (10)$$

with some constant which we have normalized, then from the equation given in the appendix for the toroidal field the angle averaged Lorentz force $\langle F_r \rangle$ for this configuration is $\langle F_r \rangle = \frac{B_0^2}{2\pi r}$. In fig. 4 we have plotted the velocity of the conversion front for the toroidal field. The nature of the curve remains same, as the angle averaged toroidal field is just six times than that of the poloidal field. Therefore a much lesser value of surface magnetic field is needed to generate the same effect in the conversion front velocity than that needed for the poloidal field. However the main factor for the toroidal field configuration remains the time and the value of the differential rotation of the star.

To summarize our results, we mention that the high magnetic field at the centre helps the front velocity to rise. For a field of dipolar nature there is an increment of about 10 percent in the front velocity. We have done a analytical calculation for different types of field configuration (in the appendix) and for a initial field of dipolar nature, and have shown our results for poloidal and toroidal configuration. It should be mentioned at this point that an earlier set of authors [35] studied the effect of an idealized configuration of the magnetic field - a constant magnetic field of moderate strength of $\sim 10^{12-13}G$ in a dipolar geometry - on the Rayleigh-Taylor (RT) instability. Through an order of magnitude estimate, they concluded that there would be a difference in the velocity of the combustion front along polar and equatorial directions. Our calculation is based on initial dipolar magnetic field with a high value of magnetic field at the center. As this is a first attempt of such kind, to have a overall understanding of the magnetic effect on propagation front, we have done averaging in the angular direction. For small value of magnetic field it is quite acceptable, but for high value of magnetic field multidimensional effect could be important. Still this method gives a good estimation of the effect of magnetic field on the propagation speed through an order of magnitude estimation. To get finer details, we need to solve general MHD equation with all multidimensional effect intact. As the exact nature of the field configuration is not known, we need to carry

out similar calculation with other forms of magnetic field. Furthermore such high magnetic fields can even modify the Einstein equation for the metric as the matter is then no longer an ideal fluid. All such a calculation is on our immediate agenda.

5. Appendix : Angle -averaged radial Lorentz force

The Lorentz force due to a magnetic field B is given by

$$\vec{F} = \frac{(\nabla \times \vec{B}) \times \vec{B}}{4\pi} \quad (11)$$

This can also be written as :

$$4\pi\vec{F} = -\frac{1}{2}\nabla(B^2) + (\vec{B} \cdot \nabla)\vec{B} \quad (12)$$

Using spherical coordinates, the radial component of the Lorentz force can be simplified as [36],

$$4\pi F_r = \nabla \cdot (B_r \vec{B}) - \frac{B_T^2}{r} - \frac{1}{2} \frac{\partial}{\partial r} (B^2) \quad (13)$$

Here, $B_T^2 = B_\phi^2 + B_\theta^2$, denotes the transverse part of the expression. The angle averaged Lorentz force is defined as:

$$\langle F_r \rangle = \int \frac{d\Omega}{4\pi} F_r \quad (14)$$

Taking the angular average of Eq (13), we get:

$$4\pi \langle F_r \rangle = \langle \nabla \cdot (B_r \vec{B}) \rangle - \frac{\langle B_T^2 \rangle}{r} - \frac{1}{2} \frac{\partial}{\partial r} (\langle B^2 \rangle) \quad (15)$$

The angle average of $\langle \nabla \cdot (\vec{B} B_r) \rangle$ can be easily evaluated. Let

$$f(r) = \langle \nabla \cdot (\vec{B} B_r) \rangle = \int \frac{d\Omega}{4\pi} \nabla \cdot (\vec{B} B_r) \quad (16)$$

Multiplying both sides by $r^2 dr$ and integrating,

$$\int dr r^2 f(r) = \int \frac{dV}{4\pi} \nabla \cdot (\vec{B} B_r). \quad (17)$$

Using Stokes theorem, the right hand side of the volume integral can be expressed as a surface integral,

$$\int dr r^2 f(r) = r^2 \int \frac{d\Omega}{4\pi} \hat{r} \cdot (\vec{B} B_r) \quad (18)$$

Now, differentiating both sides w.r.t r we get:

$$f(r) = \frac{1}{r^2} \frac{d}{dr} (r^2 \langle B_r^2 \rangle) \quad (19)$$

Using Eq (14), Eq (18) and the fact that $B^2 = B_r^2 + B_\theta^2 + B_\phi^2$, the final expression for the angle-averaged radial force can be written in terms of the angle average of the different components as:

$$4\pi \langle F_r \rangle = \frac{1}{2} \frac{d}{dr} [\langle B^2 \rangle - 2\langle B_T^2 \rangle] + \frac{2\langle B^2 \rangle - 3\langle B_T^2 \rangle}{r} \quad (20)$$

The above expression for the angle-averaged radial Lorentz force can be simplified for different magnetic field configurations some of which we enumerate below:

1. $\langle B_\theta^2 \rangle = \langle B_\phi^2 \rangle \simeq 0$ (nearly radial field):
In this case, $\langle B^2 \rangle \simeq \langle B_r^2 \rangle$. Hence

$$\langle F_r \rangle = -\frac{d}{dr} \left\langle \frac{B^2}{8\pi} \right\rangle - \frac{4}{r} \left\langle \frac{B^2}{8\pi} \right\rangle \quad (21)$$

2. $\langle B_r^2 \rangle = \langle B_\theta^2 \rangle = \langle B_\phi^2 \rangle = \frac{1}{3} \langle B^2 \rangle$:
In this case, the simplified expression is,

$$\langle F_r \rangle = -\frac{1}{3} \frac{d}{dr} \left\langle \frac{B^2}{8\pi} \right\rangle \quad (22)$$

3. $\langle B_\phi^2 \rangle = 0$ (poloidal field):
In this case, the simplified expression is,

$$\langle F_r \rangle = \frac{1}{8\pi} \frac{d}{dr} [B_r^2 - B_\theta^2] + \frac{2B_r^2 - B_\theta^2}{4\pi r} \quad (23)$$

For the special case of a dipole magnetic field, which we assume for calculations in this paper, we have

$$\langle B_r^2 \rangle = \frac{B_0^2}{r^6} \int \frac{d\Omega}{4\pi} \sin^2 \theta = \frac{2B_0^2}{3r^6}$$

$$\langle B_\theta^2 \rangle = \frac{4B_0^2}{r^6} \int \frac{d\Omega}{4\pi} \cos^2 \theta = \frac{4B_0^2}{3r^6}$$

The Lorentz force thus can be expressed as :

$$\langle F_r \rangle = \frac{B_0^2}{12\pi r^7}$$

4. $\langle B_r^2 \rangle = \langle B_\theta^2 \rangle = 0$ (toroidal field) :

In this case, the expression simplifies to:

$$\langle F_r \rangle = -\frac{d}{dr} \left\langle \frac{B_\phi^2}{8\pi} \right\rangle - \frac{B_\phi^2}{4\pi r} \quad (24)$$

For the special case of dipole field, we get

$$\langle F_r \rangle = \frac{B_0^2}{2\pi r^7}$$

R.M. thanks Grant No. SR/S2HEP12/2007, funded by DST, India for financial support. S.K.G. and S.R. thank Department of Science & Technology, Govt. of India for support under the IRHPA scheme.

References

- [1] E. Witten, Phys. Rev. D, **30**, 272 (1984)
- [2] P. Haesel, R. Schaeffer, J. L. Zdunik, Astronomy & Astrophysics, **160**, 121 (1986)
- [3] E. Farhi and R. L. Jaffe, Phys. Rev. D, **30**, 2379 (1989)
- [4] K. S. Cheng, Z. G. Dai, D. M. Wai & T. Lu, Science, **280**, 407 (1998)
- [5] S. Chin & A. K. Kerman, Phys. Rev. Lett., **43**, 1292 (1979)
- [6] M. Dey, I. Bombaci, J. Dey & B. C. Samanta, Phys. Lett. B, **438**, 123 (1998)
- [7] C. Alcock, E. Farhi and A. Olinto, Astrophys. J., **310**, 261 (1986)
- [8] N. K. Glendenning, Nucl. Phys. (Proc. Suppl.) B, **24**, 110 (1991); Phys. Rev. D, **46**, 1274 (1992)

- [9] A. Olinto, Phys. Lett. B, **192**, 71 (1987); Nucl. Phys. Proc. Suppl. B, **24**, 103 (1991)
- [10] J. Madsen and M. L. Olsen, Nucl. Phys. (Proc. Suppl.) B, **24**, 170 (1991)
- [11] G. Byam, H. Heiselberg and C. J. Pethick, Nucl. Phys. (Proc. Suppl.) B, **24**, 144 (1991)
- [12] J. Collins and M. Perry, Phys. Rev. Lett., **34**, 1353 (1975)
- [13] O. G. Benvenuto and J. E. Horvarth, Phys. Lett. B, **213**, 516 (1988)
- [14] H. T. Cho, K. W. Ng and A. W. Speliotopoulos, Phys. Lett. B, **326**, 111 (1994)
- [15] I. Tokareva, A. Nusser, V. Gurovich and V. Folomeev, Int. J. Mod. Phys. D, **14**, 33 (2005)
- [16] Z. Berezhiani, I. Bombaci, A. Drago, F. Frontera and A. Lavagno, Astrophys. J., **586**, 1250 (2003)
- [17] I. Bombaci, I. Parenti and I. Vidana, Astrophys. J., **614**, 314 (2004)
- [18] A. Drago, A. Lavagno and G. Pagliara, Phys. Rev. D, **69**, 057505 (2004)
- [19] J. Alam, S. Raha and B. Sinha, Phys. Rep., **273**, 243 (1996)
- [20] A. Bhattacharyya, S. K. Ghosh, P. Joarder, R. Mallick & S. Raha, Phys. Rev. C, **74**, 065804 (2006)
- [21] A. Bhattacharyya, S. K. Ghosh, R. Mallick & S. Raha, Phys. Rev. C, **76**, 052801 (2007)
- [22] F. C. Michel, Rev. Mod. Phys., **54**, 1 (1982)
- [23] J. Ellis, J. I. Kapusta and K. A. Olive, Nucl. Phys. B, **348**, 345 (1991)
- [24] C. Alcock E. Farhi & A. Olinto, Astrophys. J., **310**, 261 (1986)
- [25] L. D. Landau and E. M. Lifshitz, *Fluid Mechanics*, Pergamon Press (1987)
- [26] A. M. Gleeson and S. Raha, Phys. Rev. C, **26**, 1521 (1982)

- [27] R. C. Tolman, Phys. Rev., **55**, 364 (1939)
- [28] J. R. Oppenheimer and G. M. Volkoff, Phys. Rev., **55**, 374 (1939)
- [29] W. D. Arnett & R. L. Bowers, Astrophys. J. Supp., **33**, 415 (1977)
- [30] H. A. Bethe and M. Johnson, Nucl. Phys. A, **230**, 1 (1974)
- [31] C. Thompson, R. C. Duncan, Astrophys. J., **408**, 194 (1993)
- [32] J. C. Wheeler, D. L. Meier, J. R. Wilson, Astrophys. J., **568**, 807 (2002)
- [33] F.A. Rasio, S. L. Shapiro, Astrophys. J., **401**, 226 (1992)
- [34] M. Shibata, K. Uryu, Phys. Rev. D, **61**, 064001 (2000)
- [35] G. Lugones, C. R. Ghezzi, E. M. de Gouviea Dal Pino & J. E. Horvath, Astrophys. J. Lett., **581**, L101 (2002)
- [36] R. Gopal & S. Roychowdhury, JCAP, **6**,11, (2010)